Available online at www.sciencedirect.com
SCIENCE DIRECT
ELSEVIER
Ore Geology Reviews 26 (2005) 198–206
ORE GEOLOGY REVIEWS
www.elsevier.com/locate/oregeorev

# Evidence of uranium biomineralization in sandstone-hosted roll-front uranium deposits, northwestern China

Maozhong Min[a,b,*], Huifang Xu[c], Jia Chen[a], Mostafa Fayek[d]

[a]Department of Earth Sciences, State Key Laboratory of Mineral Deposit Research, Nanjing University, Nanjing 210093, People's Republic of China
[b]State Key Laboratory of Solid State Microstructures, Nanjing University, Nanjing 210093, People's Republic of China
[c]Department of Earth and Planetary Sciences, University of New Mexico, Albuquerque NM87131-1116, United States of America
[d]Department of Earth and Planetary Sciences, University of Tennessee/ORNL, TN 37996, United States of America

Received 22 September 2003; accepted 15 October 2004
Available online 25 January 2005

**Abstract**

We show evidence that the primary uranium minerals, uraninite and coffinite, from high-grade ore samples ($U_3O_8$>0.3%) in the Wuyiyi, Wuyier, and Wuyisan sandstone-hosted roll-front uranium deposits, Xinjiang, northwestern China were biogenically precipitated and psuedomorphically replace fungi and bacteria. Uranium (VI), which was the sole electron acceptor, was likely to have been enzymically reduced. Post-mortem accumulation of uranium may have also occurred through physio-chemical interaction between uranium and negatively-charged cellular sites, and inorganic adsorption or precipitation reactions. These results suggest that microorganisms may have played a key role in formation of the sandstone- or roll-type uranium deposits, which are among the most economically significant uranium deposits in the world.


*Keywords:* Roll-front uranium deposit; Sandstone; Biomineralization; China

## 1. Introduction

Reduction of U(VI) by microorganisms leading to U(IV) mineral precipitation has been extensively studied experimentally, using dilute U-bearing solutions (Lovley et al., 1991, 1996; Phillips et al., 1995; Barton et al., 1996; Tucker et al., 1998; Abdelouias et al., 1999; Panak, 2000; Haveman and Pedersen, 2002; Russell et al., 2003). Some of the first microorganisms found to reduce U(VI) were dissimilatory bacteria, such as *Geobacter metallireducens* and *Shewanella putrefaciens*, which are Fe-reducing species. These microorganisms can use U(VI) as an electron acceptor, instead of Fe(III) (Lovley et al., 1991). Several experiments have shown that reduction of U(VI) is an enzymatically

* Corresponding author. Department of Earth Sciences, State Key Laboratory of Mineral Deposit Research, Nanjing University, Nanjing 210093, People's Republic of China.
*E-mail address:* mzmin@nju.edu.cn (M. Min).

0169-1368/$ - see front matter © 2004 Elsevier B.V. All rights reserved.
doi:10.1016/j.oregeorev.2004.10.003

mediated reaction (Lovley and Phillips, 1992; Lovley et al., 1993). These experiments also showed that $HS^-$, used in these experiments to establish reducing conditions, reacts slowly with U(VI) compared with the biocatalyzed reaction, at near neutral pH and near room temperature.

Despite the above, there has been little direct evidence of biogenically precipitated U-minerals associated with uranium deposits (Milodowski et al., 1990). The objective of the present paper is to show that primary uraninite and coffinite from high-grade ore samples ($U_3O_8$>0.3%) from the Wuyiyi, Wuyier, and Wuyisan sandstone-hosted roll-front U-deposits, Xinjiang, NW China, which psuedomorphically replace fungi and bacteria, are of biogenic origin (Lowenstam, 1981).

## 2. Geologic setting

The Wuyiyi, Wuyier, and Wuyisan, roll-front uranium deposits are located along the southwest border of the YL basin, Xinjiang, NW China. A detailed geological setting for these deposits has been previously given by Min et al. (2001, 2005). The YL Basin covers an area of approximately 16,000 $km^2$ (Fig. 1a) and is a closed continental basin that has an approximately NW–SE trend. Basement rocks of the YL Basin consist of Proterozoic metasediments, Carboniferous intermediate-acidic volcanic and volcaniclastic rocks, and Hercynian age granites. Cap rocks of the basin comprise Triassic, Jurassic, Cretaceous, and Tertiary conglomerates, sandstones and pelites, Jurassic coal, and Quaternary gravel, sand and clay. The oldest rocks exposed in the Wuyiyi, Wuyier, and Wuyisan ore districts are metamorphosed quartzite, marble, carbonaceous slate of the Middle Proterozoic, which are unconformably overlain by Lower Palaeozoic conglomerates, sandstones, pelites and limestones. The Carboniferous intermediate-acidic volcanic rocks rest unconformably on conglomerates, sandstones, pelites and limestones of the Lower Palaeozoic, which are, in turn, unconformably overlain by sandstones and pelites of the Upper Triassic Xiaoquangou Group. The latter are conformably overlain by conglomerates, sandstones, pelites and coal of the Lower–Middle Jurassic Shuixigou Group. The Upper Cretaceous red conglomerates and sandstones lie conformably on top of the Lower–Middle Jurassic Shuixigou Group, which are conformably overlain by the Tertiary red conglomerates, sandstones and pelites, which are unconformably overlain by Quaternary gravel, sand and clay.

The three deposits in question occur in the lower to middle units of the continental Jurassic Shuixigou Group. Ore-bearing rocks of the Jurassic Shuixigou Group dip to the northeast. The thickness of the Shuixigou Group ranges from 220 to 440 m and can be divided into three members. These are, from bottom to top, the Badaowan Formation, which lies unconformably over the Xiaoquangou Group (Middle–Upper Triassic), the Sangonghe Formation, which lies conformably on top of the Badaowan Formation, and the Xishanyao Formation, which lies conformably on top of the Sangonghe Formation. Uranium mineralization occurs within five distinct stratigraphic horizons, all of which follow the inner margin of the basin.

The uranium orebodies consist of medium- to coarse-grained sandstone and occur at the location of an abrupt change in redox conditions. On the up-dip side of the roll-front and tabular-shaped ore bodies, the host sandstone is highly oxidized, yellowish orange to red in color, lacks pyrite, and has little carbonaceous debris. These oxidized tongues of sandstone can extend for tens of kilometers. Ore samples are gray, dark gray or black in color. Uranium-rich rocks are often enriched in molybdenum and vanadium, and are commonly in sharp contact with barren altered rocks. Principal epigenetic metallic minerals in the ores, from oldest to youngest, are hematite, sphalerite, pyrite, marcasite, uraninite and coffinite. There is abundance of fossilized wood fragments associated with the ore bodies. Some of wood fragments were mineralized, where uraninite and coffinite preserve the original wood-cell texture (Min et al., 2001). The U-mineralization gives young whole-rock U–Pb isotope ages, ranging from 11.7±0.3 Ma to 15.8±0.4 Ma (Min et al., 2001). The timing of uranium mineralization for the deposits therefore corresponds with the Himalayan (Late Tertiary) tectonism that affected the northwest region of China.

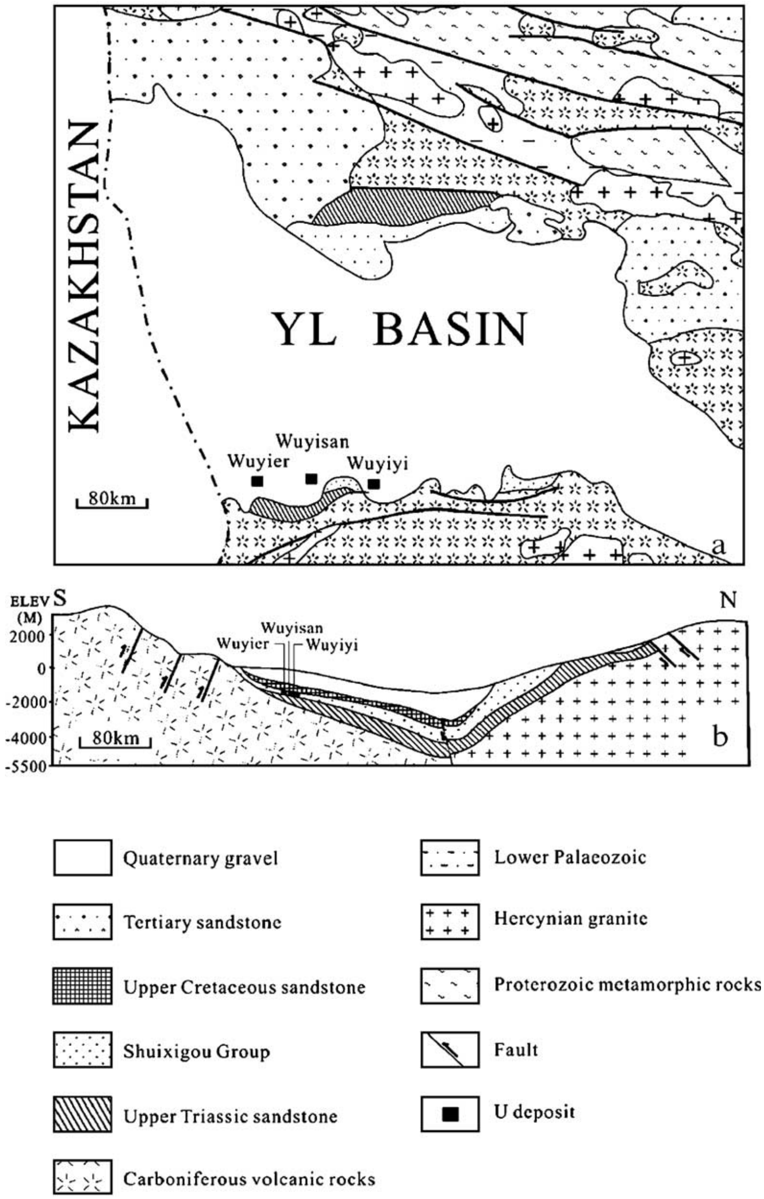


Fig. 1. Regional geological setting (a) and North–South geological cross-sections (b) of the Wuyiyi, Wuyier, and Wuyisan uranium districts in the YL Basin (modified after 216 Geological Party, 1997).

The deposits are genetically similar to sandstone-hosted roll-front U-deposits found in the Colorado plateau, southern Texas, the Tertiary Basin of Wyoming and the Ambrosia Lake of New Mexico, USA (Granger et al., 1961; Dahl and Hagmaier, 1974; Reynolds and Goldhaber, 1982), the East Kalkarod, Goulds Dam, Honeymoon and Manyingee districts, Australia (IAEA, 1996), Irkol, Kanzhugan, Kyztu, Mynkuduk and Uvanas in Kazakhstan, Folakara, Madagascar, La Sierrita, Mexico, and the Agron, Aktau, Bukeenai and Uchkuduk districts of Uzbekistan (IAEA, 1996).

## 3. Methodology

Ore samples were selected from drillholes that intersect uraniferous orebodies in the Wuyiyi, Wuyier, and Wuyisan deposits. Polished thin sections were examined using optical microscopy, electron microprobe, scanning electron microscopy and scanning transmission electron microscopy (STEM) to determine mineral paragenesis and textures. SEM analyses of uranium minerals and fossilized microorganisms were made using a JEOL JSM-5800LV instrument at the Department of Earth and Planetary Sciences, University of New Mexico, USA. Chemical compositions of fossilized microorganism were determined with an X-ray EDS analyzer on the SEM. TEM analyses and electron diffraction studies were carried out using JEOL JEM-2010 HRTEM and Phillips 420 FEG XRD instruments, respectively, both located at the Department of Earth and Planetary Sciences, University of New Mexico, USA.

## 4. Results

SEM analyses indicate that the primary U-minerals, uraninite ($UO_2$) and coffinite ($USiO_4$), have pseudomorphs after microbe in the ore samples (Figs. 2 and 3). Uraninite within the fossilized wood pseudomorphically replaces branching dendritic hyphae and globular fungi spores (Figs. 2a–d). Individual hyphae have a tubular structure (Fig. 2d). The size of the uraninite-mineralized hyphae and spores ranges from 0.2 to 0.5 μm and from 0.5 to 1.2 μm across, respectively. EDS analysis shows that the hyphae and spores have a simple chemical composition (uraninite, $UO_2$; Fig. 2b).

The coffinite-mineralized worm-like bacteria have a length of 1.7 to 2.2 μm, and an average width of 0.3 μm (Fig. 3a). EDS analyses indicate that the worm-like bacteria contain U and Si (coffinite, $USiO_4$; Fig. 3b). Almost all uraninite in the ores surrounding the fossilized wood has a structure resembling globular cocci with diameters of 2 to 3 μm and occurs as botryoidal aggregate on surfaces of the organic debris (Fig. 3c).

Structures resembling nano-scale organisms replaced by $UO_2$ (uraninite) were detected using HRTEM imaging (Fig. 3d). Although identification of these organisms is beyond the scope of this study, these organisms are 20 to 25 nm in length and have an average width of 8 nm. Electron diffraction patterns of selected area (lower left inserted in Fig. 3d) show a large number of uraninite nano-crystals, which are arranged in ordered three-dimensional arrays.

Framboidal pyrite commonly occurs within the matrix of the uranium minerals and within the fossilized wood cells (Fig. 3e), and is an early diagenetic mineral. It is a spherical to sub-spherical aggregates of equigranular microcrystals. The average diameter of the spherical framboid is between 10 and 12 μm. Within individual framboids, microcrystals are remarkably uniform in size (10 μm across) and shape and are often arranged in ordered three-dimensional arrays (Fig. 3e). SEM investigations indicate that ratio of the framboid diameter to microcrystal diameter is generally between 20 and 25. The packing arrangement of the microcrystals is typically dense, approaching cubic closest packing. The framboidal pyrite is commonly replaced by uranium (Fig. 3f). It is indicated that U can partially be reduced by sulfur in pyrite that is earlier than uraninite. Electron diffraction patterns of the framboidal pyrite (Fig. 3e) show that there is abundant uraninite present.

## 5. Discussion and conclusions

The uranium cycle near the Earth's surface is mainly controlled by redox reactions. Sandstone-hosted or roll-front U-deposits are the most abundant uranium reservoirs in the world (Degens and Ittekkot, 1982; Langmuir, 1978; Suzuki and Banfield, 1999), and are also economically the most important U-resources in China. Precipitation mechanisms for U(VI) in roll-front U-deposits are controversial. The conventional view is that U(VI) reduction is due to an inorganic reaction in which sulphide, molecular hydrogen or organic compounds function as the reductants (e.g., Nash et al., 1981; Langmuir, 1978; Charles, 1996; Suzuki and Banfield, 1999).

Preservation of microfossils in the Wuyiyi, Wuyier, and Wuyisan uranium deposits was likely due to binding between U and microbial cells (e.g., Gravesen et al., 1994). Sandstone-hosted U-deposits contain abundant organic material ($C_{org}$=0.1 to 2.1 wt.%), and formed by reduction of U(VI) to insoluble U(IV) at

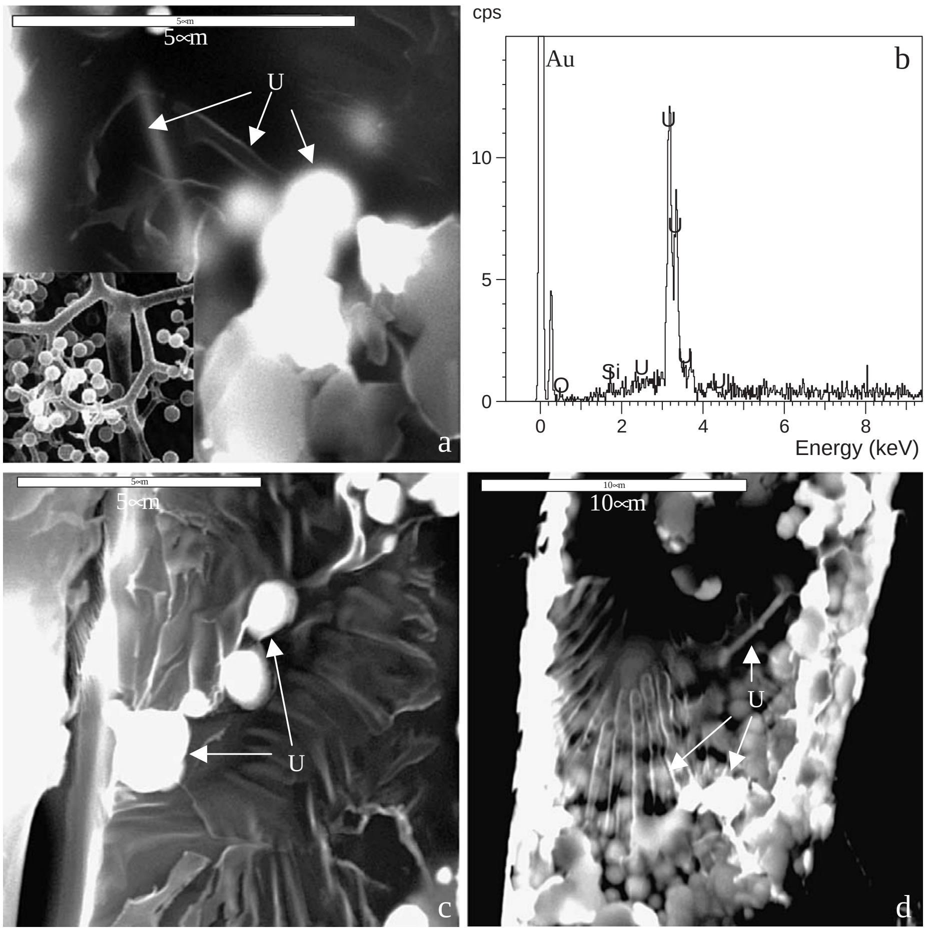


Fig. 2. (a) SEM micrograph showing morphology of branching dendritic hyphae (white, U) and globular spores (white, U) of fungi, which were entirely replaced by $UO_2$ (uraninite) within fossilized wood cell-holes of the ore from the Wuyisan deposit. Insert (lower left corner) is modern fungi (Gravesen et al., 1994). (b) EDS-spectrum from the hyphae and spores in (a), (c), (d). Au peaks result from the Au grid. (c) SEM micrograph showing morphology of globular spores (white, U) and (gray white, U) fungi, which were entirely replaced by $UO_2$ (uraninite), as shown in (b), and within fossilized wood cell-holes of the ore from the Wuyisan deposit. (d) SEM micrograph showing morphology of aggregated tubular hyphae (gray white, U) and globular spores (white, U), entirely replaced by $UO_2$ (uraninite), as shown in Fig. (b). Sample is from the Wuyiyi deposit.

relatively low-temperatures of 40 to 50 °C (Suzuki and Banfield, 1999; Min et al., 2003). Low-temperature, organic rich environments in sandstones have been shown, experimentally, to be suitable for growing various microorganisms that can enzymatically reduce U(VI) to U(IV) (Lovley and Phillips, 1992). In particular, the fossilized wood cells in the host sandstone are ideal environments for growth of microorganisms because the wood supplies both a source of nourishment and space necessary for growth.

The results of this study strongly suggest that U-reduction in the Wuyiyi, Wuyier, and Wuyisan roll-front deposits was due to U-metal–organic material interaction and microbially-mediated reactions. Both bacteria and fungi were likely responsible for U-reduction. During the initial stage of mineralization, living bacteria enzymatically reduced and accumulated U(VI) in the host sandstones, and grew using U(VI) as the sole electron acceptor (Lovley et al., 1991). This metabolism-dependent U accumulation consists of extracellular (outer membrane) precipita-

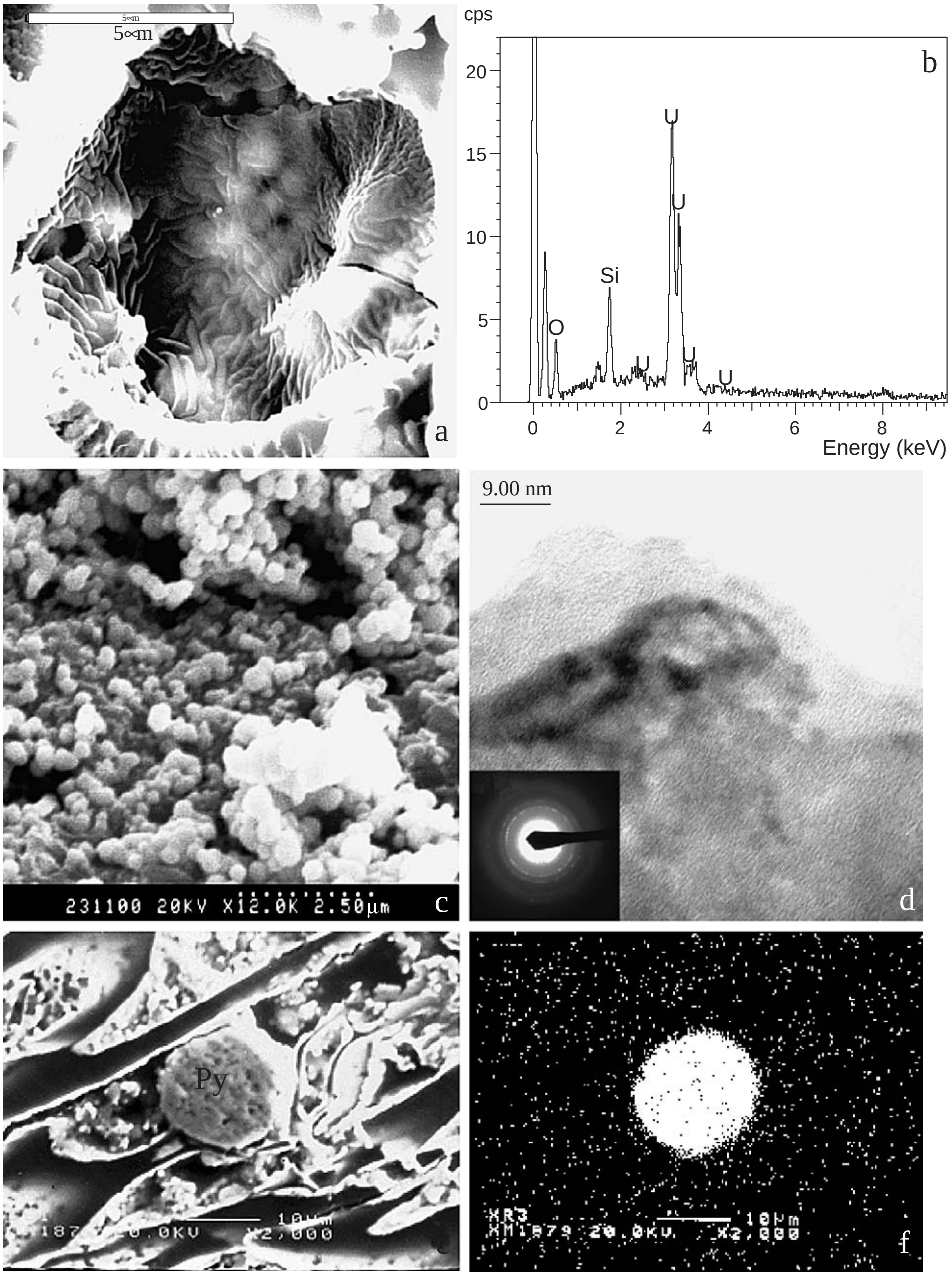


Fig. 3. (a) SEM micrograph showing the morphology of worm-like bacteria (*Desulfovibrio desulfuricans*?), completely replaced by $USiO_4$(coffinite) in a fossilized wood cell of the sandstone-hosted uranium ore from the Wuyiyi deposit. (b) EDS spectrum from the worm-like bacteria in (a). Au peaks result from the Au grid. (c) SEM micrograph showing morphology of globular cocci, entirely replaced by $UO_2$ (uraninite), and of botryoidal structure on surface of mineral clastics in the ore from the Wuyier deposit. (d) HRTEM micrograph showing morphology of a structure resembling nano-organism replaced by $UO_2$ (uraninite nano-crystals, black). Inserted small pattern (lower left) is from the uraninite nano-crystals. Sample is from the Wuyiyi deposit. (e) SEM micrograph showing morphology of framboidal pyrite (Py) in the fossilized wood cell. (f) X-ray emission image of the same view as in (e), for element U.

tion with metabolically-produced ligands, complexation arising from excreted metabolites, and precipitation due to enzyme-mediated changes in the redox state (Gadd, 1996; Suzuki and Banfield, 1999). Uranium uptake by fungi was attributed to complexation with nitrogen at chitin amine binding sites in the cell wall, subsequently adsorbed within the chitin matrix, and deposition of uranyl hydroxide (Tsezos and Volesky, 1982). When amounts of accumulated U(VI) increased on the cell walls, the microorganisms eventually died due to U toxicity and high radiation doses.

However, U accumulation did not stop once the cells died. Replacement of fungi and bacteria by uranium minerals suggest that post-mortem accumulation of U was likely most important in the formation of the biogenic uraninite and coffinite in the roll-front deposits under discussion. Post-mortem accumulation of U usually occurs between uranium species and negatively charged sites in the non-living microorganisms (Suzuki and Banfield, 1999), or by inorganic adsorption and precipitation reactions, where the microorganism is eventually replaced by the U-bearing phase. The framboidal pyrite commonly occurs in the matrix of the U ores, within the fossilized wood cells (Fig. 3e), and along cleavages of the clastic minerals, such as biotite and feldspar. The framboidal texture and close association with carbonized, fossilized plant fragments implies an in situ biogenic origin due to bacterial sulfate reduction (Northrop and Goldhaber, 1990). Recent studies support this observation because they show that control over pyrite morphology is related to the amount and reactivity of the organic matter within the deposited sediments (Abdelouias et al., 1999). Butler and Rickard (2000) and Taylor and Macquaker (2000) show that framboidal pyrite precipitates from Fe-dominated fluids in the region of organic matter as a result of bacterial sulfate reduction where, locally, sulfide production rates are high enough for the fluids to reach strong supersaturation with respect to FeS. Euhedral (non-framboidal) pyrite forms from iron-dominated fluids in which sulfide production rate is such that FeS saturation is not reached. Additionally, detailed examination of the framboid-like pyrite reveals that a strong correlation between pyrite morphologies and the presence of (or amount of introduced) $S^0$ exists. In the presence of excess $S^0$, pyrite morphologies changed from euhedral and framboid-like to spheroidal or acicular aggregates.

The observations made in this study suggest that microorganisms have played a key role in formation of roll-front Wuyiyi, Wuyier, and Wuyisan U-deposits, China. In addition to U, Mo, Se and Rh are also associated with these deposits as by-products, and spatially have a zoned distribution in the C-shaped roll-front ore bodies (Jensen, 1958; Reynolds and Goldhaber, 1982; Northrop and Goldhaber, 1990). This spatial distribution of U, Mo, Se and Re in the sandstone-hosted roll-front U ores may be due to spatially distributed anaerobic microorganisms that can selectively enzymatically U, Mo, Se and Re (Tucker et al., 1998; Xu et al., 2000).

The potential for U contamination of surface- and groundwaters through mining and milling operations, spent fuel reprocessing, disposal of nuclear wastes and nuclear explosion is an environmental concern. The results presented here suggest that large-scale microbial remediation of U is possible. Other radioactive metals, such as Pu and Tc in high-level radioactive waste, have multiple redox states, similar chemical behaviors to U, and are insoluble in the reduced form. Therefore, these radionuclides can also be microbially sequestered. Uptake and precipitation of U and other radionuclides by microorganisms may be a cost-effective method of radionuclide remediation. However, to effectively use microorganisms to remediate heavy metal and radionuclide contaminated subsurface environments, more work is required to isolate and culture those microorganisms associated with highly radioactive environments, such as U-deposits and associated mining and milling operations, because these microorganisms are likely able to reduce and accumulate far larger quantities of U over a wider range of pH conditions than microorganisms from uncontaminated sites (Wade and DiChristina, 2001).

## Acknowledgements

We thank scientists at Department of Earth and Planetary Sciences, University of New Mexico (USA) for their technical support. This work was supported by the National Natural Science Foundation of China (NNSFC, Grant No. 40173031), the International

Cooperative Research Foundation of NNSFC (Grant No.2002-40210104086) and Ph.D. Base Foundation of Chinese Education Ministry (Grant no. 20020284036). The manuscript benefited considerably from critical reviews and helpful comments by Nigel Cook and two anonymous reviewers.

## References

216 Geological Party, 1997. Geological report of the Wuyiyi uranium deposit. Unpublished geological report (in Chinese), p. 6–10.

Abdelouias, A., Lutze, W., Nuttall, H.E., 1999. Oxidative dissolution of uraninite precipitated on Navajo sandstone. Journal of Contaminant Hydrology 36, 353–375.

Barton, L.L., Choudhury, K., Thomson, B.M., Steenhoudt, K., Groffman, A.R., 1996. Bacterial reduction of soluble uranium: the first step of in situ immobilization of uranium. Radioactive Waste Management and Environmental Restoration 20, 141–145.

Butler, I.B., Rickard, D., 2000. Framboidal pyrite formation via the oxidation of iron (II) monosulfide by hydrogen sulphide. Geochimica et Cosmochimica Acta 64, 2665–2672.

Charles, S., 1996. The roles of organic matter in the formation of uranium deposits in sedimentary rocks. Ore Geology Reviews 11, 53–59.

Dahl, A.R., Hagmaier, J.L., 1974. Genesis and characteristics of the southern Power River basin uranium deposits, Wyoming, USA. Formation of Uranium Ore Deposits. International Atomic Energy Agency, Vienna, pp. 201–216.

Degens, E.T., Ittekkot, V., 1982. In situ metal-staining of biological membranes in sediments. Nature 298, 262–264.

Gadd, G.M., 1996. Influence of microorganisms on the environmental fate of radionuclides. Endeavour 20, 150–156.

Granger, H.C., Santos, E.S., Dean, B.G., Moore, F.B., 1961. Sandstone-type uranium deposits at Ambrosia Lake, New Mexico—an interim report. Economic Geology 56, 1179–1209.

Gravesen, S., Frisvad, J.C., Samson, R.A., 1994. Fungi. Special-Trykkeriet Viborg, Denmark. 156 pp.

Haveman, S.A., Pedersen, K., 2002. Microbially mediated redox processes in natural analogues for radioactive waste. Journal of Contaminant Hydrology 55, 161–174.

IAEA, 1996. Guidebook to Accompany IAEA Map: World Distribution of Uranium Deposits. Vienna, p. 20–210.

Jensen, M.L., 1958. Sulfur isotopes and the origin of sandstone-type uranium deposit. Economic Geology 53, 598–616.

Langmuir, D., 1978. Uranium solution–mineral equilibria at low temperatures with applications to sedimentary ore deposits. Geochimica et Cosmochimica Acta 42, 547–569.

Lovley, D.R., Phillips, E.J.P., 1992. Reduction of uranium by *Desulfovibrio desulfuricans*. Applied and Environmental Microbiology 58, 850–856.

Lovley, D.R., Phillips, E.J.P., Gorby, Y.A., Landa, E.R., 1991. Microbial reduction of uranium. Nature 350, 413–416.

Lovley, D.R., Roden, E.E., Phillips, E.J.P., Woodward, J.C., 1993. Enzymatic iron and uranium reduction by sulfate-reducing bacteria. Marine Geology 113, 41–53.

Lovley, D.R., Coates, J.D., Blunt-Harris, E.L., Phillips, E.J.P., Woodward, J.C., 1996. Humic substances as electron acceptors for microbial respiration. Nature 382, 445–448.

Lowenstam, N.A., 1981. Minerals formed by organisms. Science 211, 1126–1130.

Milodowski, A.E., West, J.M., Pearce, J.M., Hyslop, E.K., Basham, I.R., Hooker, P.J., 1990. Uranium-mineralized microorganisms associated with uraniferous hydrocarbons in southwest Scotland. Nature 347, 465–467.

Min, M.Z., Luo, X.Z., Mao, S.L., Wang, Z.Q., Wang, R.C., Qin, L.F., Tan, X.L., 2001. An excellent fossilized wood cell texture with primary uranium minerals at a sandstone-hosted roll-type uranium deposit, NW China. Ore Geology Reviews 17, 233–239.

Min, M.Z., Wang, R.C., Bian, L.Z., 2003. Biomineralization in sandstone-hosted interlayer oxidation-zone type uranium deposits. Progress in Natural Science 13, 164–168 (in Chinese).

Min, M.Z., Chen, J., Wei, G.H., Fayek, M., 2005. Mineral paragenetic associations and textural pattern in sandstone-hosted roll-type uranium deposits, northwestern China. Ore Geology Reviews (in press).

Nash, J.T., Granger, H.C., Adams, S.S., 1981. Geology and concepts of genesis of important type of uranium deposits. Economic Geology 75, 63–116.

Northrop, H.R., Goldhaber, M.B., 1990. Genesis of the tabular-type vanadium–uranium deposits of Herry basin, Utah. Economic Geology 85, 215–269.

Panak, P.J., 2000. Complex formation of U (VI) with *Bacillus*-isolates from a uranium mining waste pile. Radiochimica Acta 88, 71–85.

Phillips, E.J.P., Lovely, D.R., Landa, E.R., 1995. Remediation of uranium contaminated soils with biocarbonate extraction and microbial U(VI) reduction. Journal of Industrial Microbiology 14, 203–206.

Reynolds, R.L., Goldhaber, M.B., 1982. Biogenic and nonbiogenic ore-forming processes in the South Texas U district: evidence from the Panna Maria deposit. Economic Geology 77, 541–556.

Russell, R.A., Holden, P.J., Wilde, K.L., Neilan, B.A., 2003. Demonstration of the use of Scenedesmus and Carteria biomass to drive bacterial sulfate reduction by *Desulfovibrio alcoholovorans* isolated from an artificial wetland. Hydrometallurgy 71, 227–234.

Suzuki, Y., Banfield, J., 1999. Geomicrobiology of uranium. In: Burns, P.C., Finch, R. (Eds.), Uranium: Mineralogy, Geochemistry and the Environment, Reviews in Mineralogy, vol. 38, pp. 393–432.

Taylor, K.G., Macquaker, J.H.S., 2000. Early diagenetic pyrite morphology in a mudstone-dominated succession: the Lower Jurassic Cleveland Ironstone Formation, eastern England. Sedimentary Geology 131, 77–86.

Tsezos, M., Volesky, B., 1982. The mechanisms of uranium biosorption by *Rhizopus arrhizus*. Biotechnology and Bioengineering 24, 385–401.

Tucker, M.D., Barton, L.L., Thompson, B.M., 1998. Reduction of Cr, Mo, Se, and U by *Desulfovibrio desulfuricans* immobilized in polacrylamide gels. Journal of Industrial Microbiological Biotechnology 20, 13–19.

Wade Jr., R., DiChristina, T.J., 2001. Isolation of U(VI) reduction-deficient mutants of *Shewanella putrefaciens*. FEMS Microbiology Letters 184, 143–148.

Xu, H., Barton, L.L., Zhang, P., Wang, Y., 2000. TEM investigation of $U^{6+}$ and $Re^{7+}$ reduction by *Desulfovibrio desulfuricans*, a sulfate-reducing bacterium. Scientific Basis for Nuclear Waste Management 23, 365–371.